Supplement of Solid Earth, 10, 809–838, 2019
https://doi.org/10.5194/se-10-809-2019-supplement

Solid Earth
Open Access

Supplement of

Fluid-mediated, brittle–ductile deformation at seismogenic depth – Part 1: Fluid record and deformation history of fault veins in a nuclear waste repository (Olkiluoto Island, Finland)

Barbara Marchesini et al.

Correspondence to: Barbara Marchesini (barbara.marchesini2@unibo.it, barbaramarchesini@hotmail.it) and Giulio Viola (giulio.viola3@unibo.it)

EBSD analysis

Before EBSD analysis, thin sections were chemically polished using colloidal silica. Thin sections were then carbon coated placed in a JEOL 6610 SEM equipped with a Nordlys Nano EBSD detector, at a 70° tilt to the horizontal (Prior et al., 1999). We used 20 kV of accelerating voltage, a working distance of 25 mm and a step size to 2 µm. The acquired EBSD patterns were automatically indexed using AZtec software and processed using CHANNEL 5 software from Oxford Instruments. Raw indexing of the two acquired maps was 96%. EBSD data were presented in the form of Inverse Pole Figure maps oriented with respect to the direction perpendicular to the vein wall (direction X0, vein wall corresponds to direction Y0), and of pole figures (equal area, lower hemisphere) oriented parallel to the Y0-X0 plane. Crystallographic data in the pole figures are plotted as one-point-per-pixel. In the IPF maps, low-angle boundaries (misorientation between 2°and 10°) are shown in cyan, high-angle boundaries (misorientation > 10°) are shown in black, and Dauphinétwin boundaries (misorientation of 60° around the c-axis) are shown in red.

Supplementary Figures:

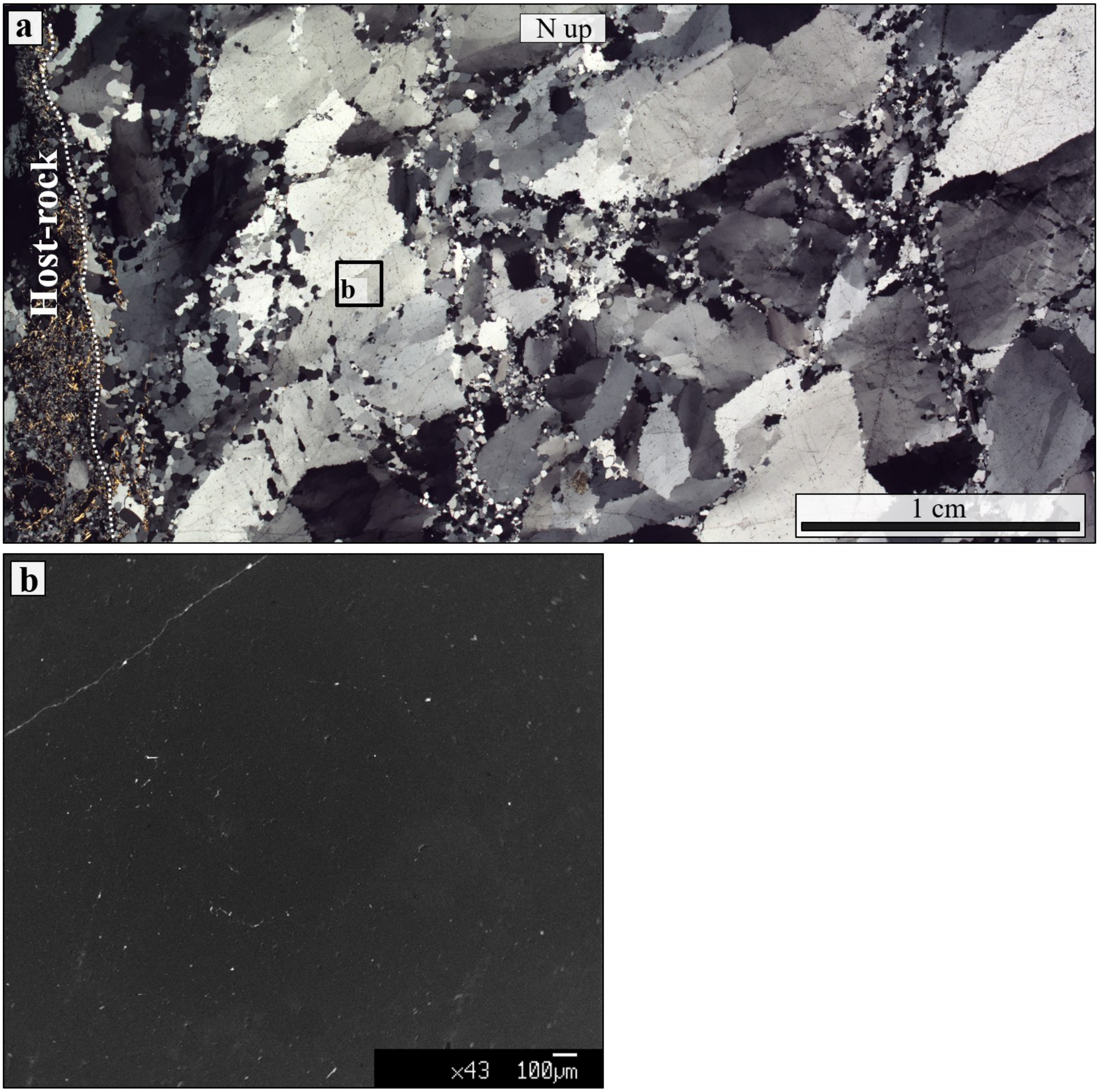

Figure S1. Stitched photomicrographs of fault core Qtz I where the location of the catodoluminescence imaging is reported. b) Panchromatic cathodoluminescence image of intercrystalline fracture occurring within Qtz I from the fault core, showing homogeneous-dark signal.

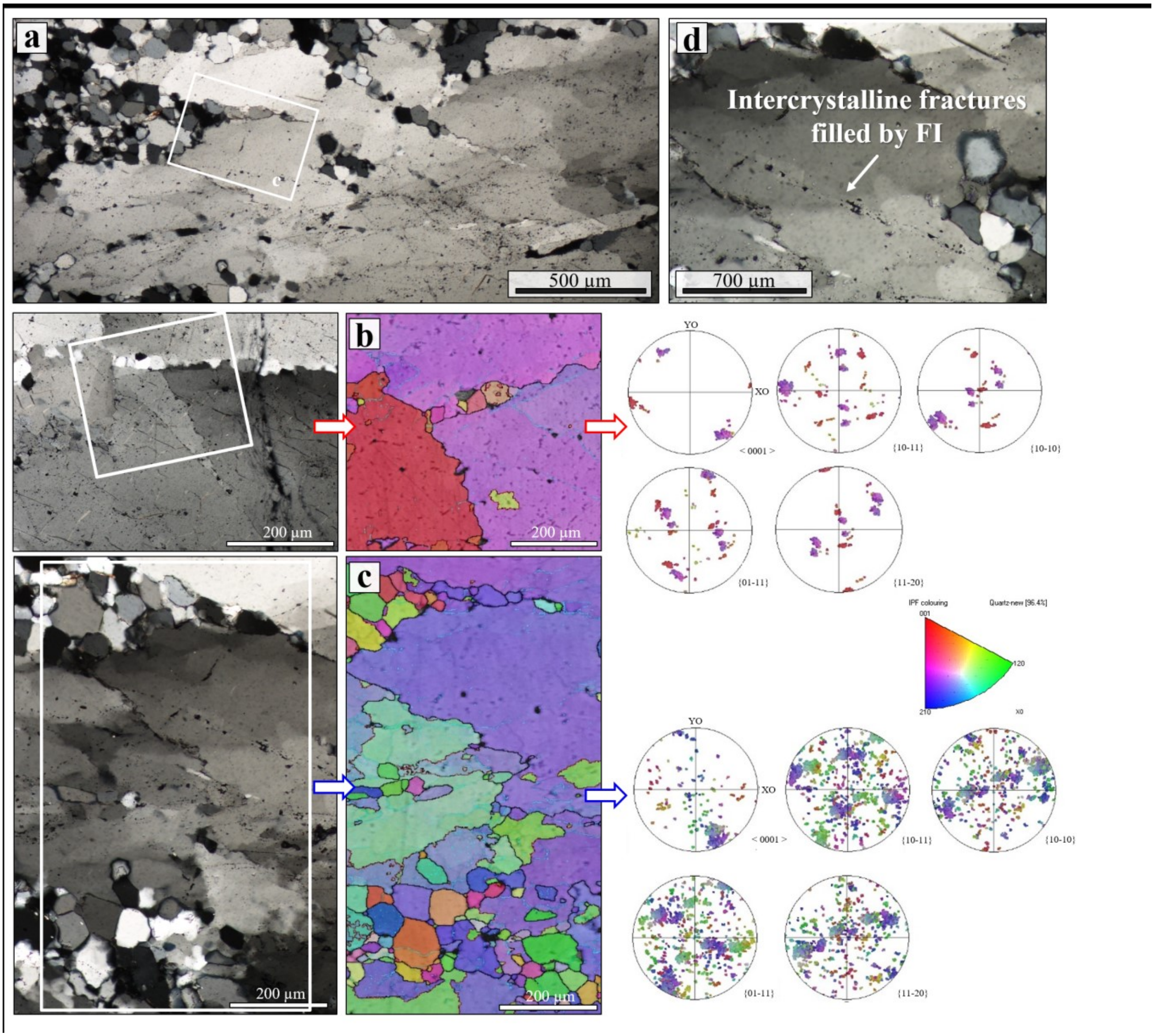

Figure S2. EBSD analysis performed on fault core-Qtz I (sample TPH-120 4). a) Qtz I-fault core microstructures where EBSD map locations b) and c) are also reported. Also at the edge of intercrystalline bands we detected subgrains precursors of recrystallization. d) Intercrystalline bands are also marked by trails of fluid inclusions

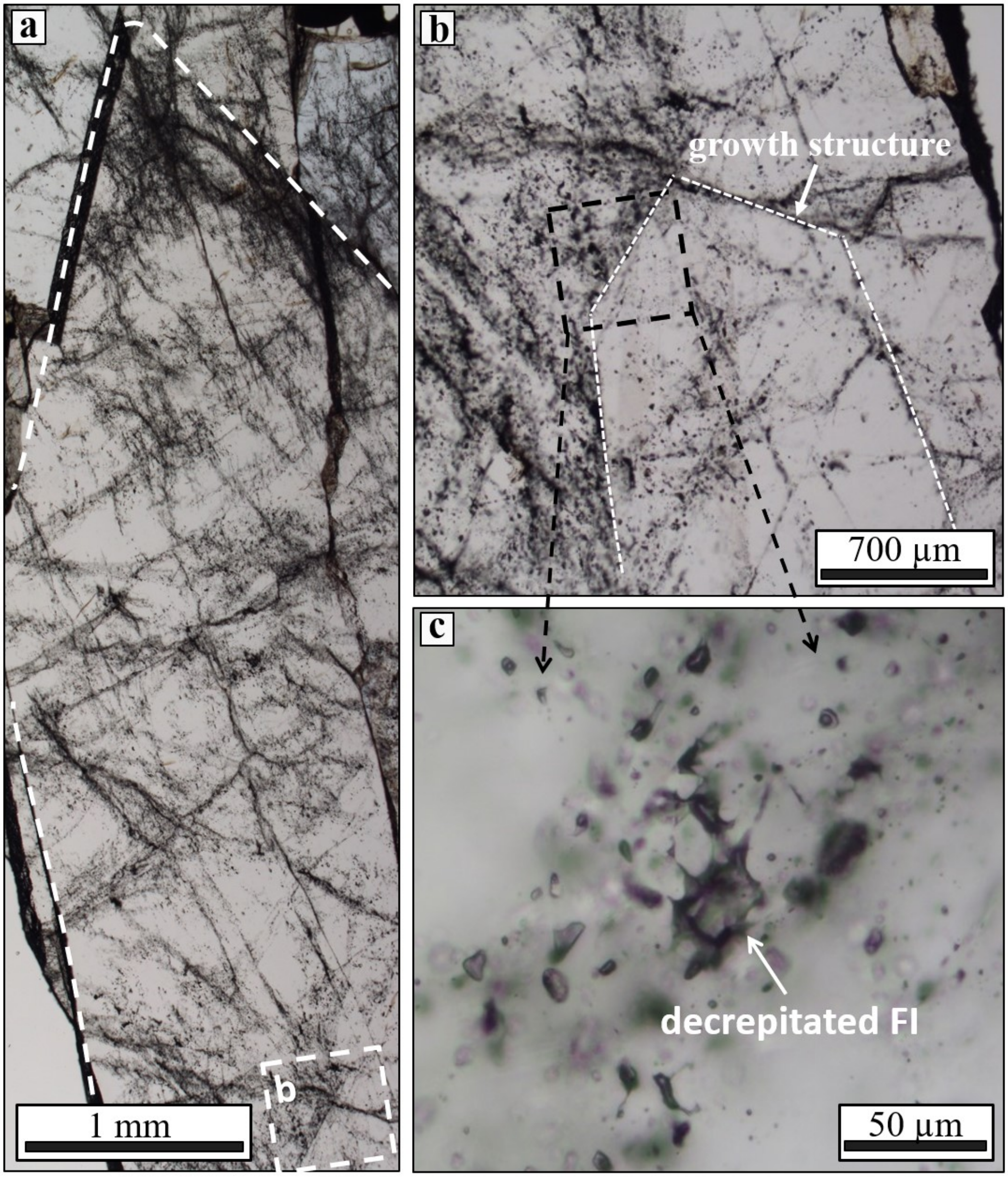

Figure S3. Petrographic relationships between fluid inclusions and Qtz II (sample TPH-120-6). a) Optically continuous, single crystal (highlighted). The white dashed square at the bottom right corner marks a possibly primary FIA entrapped during crystal growth. b) Enlargement of the growth structure. c) Enlargement of a portion of the primary growth zone, showing a re-equilibrated cluster of fluid inclusions along the primary growth zone. Note that the largest fluid inclusion is decrepitated and is surrounded by planes of tiny and irregular FIs (satellite inclusions). In the light of this structures, microthermometric estimations from this thype of assemblages are excluded.

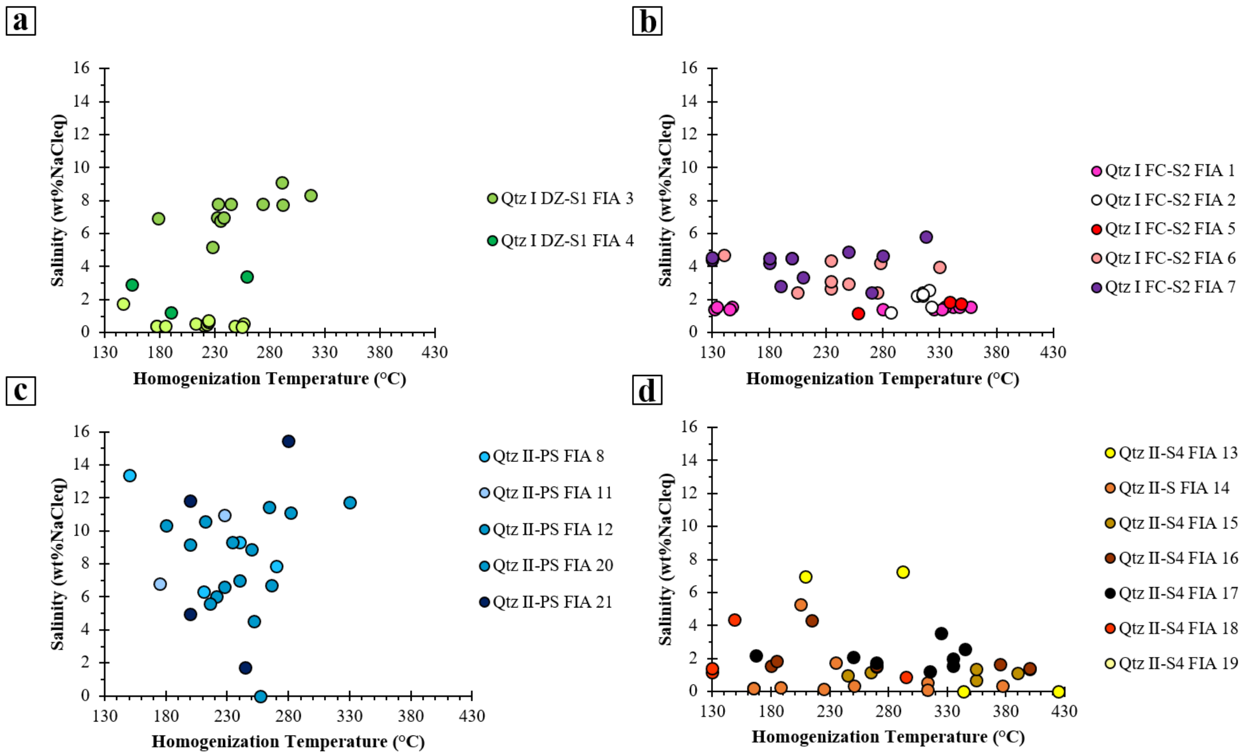

Figure S4. Homogenization Temperature vs. Salinity plots for fluid inclsuions types identified in each structural domain: a) Qtz I-damage zone; b) Qtz I-fault core; c) Pseudosecondary FI in Qtz II-fault core; d) secondary FI entrapped within Qtz II vein. These plots are used to estimate the most probable composition of the fluids.